

Upper critical field, penetration depth and depinning frequency of the high-temperature superconductor $\text{LaFeAsO}_{0.9}\text{F}_{0.1}$ studied by microwave surface impedance.

A. Narduzzo,¹ M. S. Grbić,² M. Požek,² A. Dulčić,² D. Paar,^{1,2} A. Kondrat,¹ C. Hess,¹
I. Hellmann,¹ R. Klingeler,¹ J. Werner,¹ A. Köhler,¹ G. Behr¹ and B. Büchner.¹

¹*Institute for Solid State Research, IFW Dresden, D-01101 Dresden, Germany; and*

²*Department of Physics, Faculty of Science, University of Zagreb, P. O. Box 331, HR-10002 Zagreb, Croatia.*

(Dated: February 2, 2022)

Temperature and magnetic field dependent measurements of the microwave surface impedance of superconducting $\text{LaFeAsO}_{0.9}\text{F}_{0.1}$ ($T_c \approx 26\text{K}$) reveal a very large upper critical field ($B_{c2} \approx 56\text{T}$) and a large value of the depinning frequency ($f_0 \approx 6\text{GHz}$); together with an upper limit for the effective London penetration depth, $\lambda_{\text{eff}} \leq 200\text{nm}$, our results indicate a strong similarity between this system and the high- T_c superconducting cuprates.

PACS numbers: 74.25.Nf, 74.25.Op, 74.25.Qt.

Keywords: microwave response, upper critical fields, penetration depth.

The recent discovery of superconductivity in $\text{LaFeAsO}_{0.9}\text{F}_{0.1}$ ¹ has lead to the rapid growth in the number of superconducting layered oxypnictides with larger and larger T_c ($\approx 55\text{K}$ in $\text{SmO}_{0.8}\text{F}_{0.2}\text{FeAs}$).² Apart from their high T_c , the interest in these materials stems primarily from the proximity of superconductivity to a spin-density-wave (SDW) ground state, and from the fact that multiple bands resulting from the orbitals of the conventionally pair-breaking magnetic ion Fe^{2+} appear to be here directly responsible for the formation of the superconducting condensate. Both *ab initio* band structure and LDA calculations^{3,4,5,6} show that the Fe-pnictide layers are responsible for the (super)conductivity; specifically, the $3d$ orbitals of the Fe^{2+} ions weakly hybridized with the As^{3-} $4p$ orbitals, form two electron and two hole pockets, while the $[\text{RE}(\text{OF})]$ ($\text{RE} = \text{La}, \text{Pr}, \text{Ce}, \text{Sm}$) layers act as charge reservoirs, F^{1-} causing the electron doping, the size of the RE element generating chemical pressure. The electronic structure thus consists of multiple quasi-two-dimensional Fermi surface sheets in the presence of competing ferromagnetic and antiferromagnetic fluctuations.^{4,6} The microscopic nature of the superconducting pairing and the symmetry of the order parameter on the other hand are still far from established, with theoretical proposals ranging from extended s-wave mediated by antiferromagnetic spin fluctuations³ to spin-triplet p -wave.⁷ The possibility of anomalously strong electron phonon coupling effects has also been emphasized,⁸ while a very small value of the electron-phonon coupling constant ($\lambda_{\text{e-ph}} < 0.21$ has been calculated.⁹ The expected large moment for the undoped compound ($S = 2$) is experimentally not observed, low temperature values of $\mu \approx 0.36\mu_B$ ¹⁰ and $\mu \approx 0.25\mu_B$ ¹¹ being reported instead. In this parent compound a structural phase transition from tetragonal to orthorhombic occurs at $T_s \approx 150\text{K}$, closely related to the formation of a spin-density-wave (SDW) below $T_N \approx 135\text{K}$. Electron doping rapidly suppresses both structural and SDW transitions leading

to superconductivity, possibly allowing short-range magnetic fluctuations to survive in the region of the phase diagram where superconductivity becomes the preferred ground state. Whether or not these local fluctuations are responsible for the pairing is here the fundamental question. Further evidence for possible unconventional pairing with nodal order parameter comes from specific heat,¹² tunneling,¹³ magnetisation¹⁴ and NMR¹⁵ measurements.

Here we report on temperature ($4.2\text{K} < T$) and magnetic field dependence ($\mu_0 H < 16\text{T}$) of the microwave surface impedance of $\text{LaFeAsO}_{0.9}\text{F}_{0.1}$. The results allow us to estimate the upper critical field B_{c2} , the effective London penetration depth λ_{eff} and the depinning frequency f_0 for this material.

Polycrystalline samples of $\text{LaFeAsO}_{0.9}\text{F}_{0.1}$ were prepared by a solid state reaction method and annealed in vacuum.¹⁶ Inspection with a polarized light microscope revealed dense crystallites of sizes varying between 1 and 100 μm . The resistivity of the sample under study was measured by means of a standard DC method with four-point contact geometry and current polarity inversion. The magnetic susceptibility, both zero-field (ZFC) and field cooled (FC), was measured using a SQUID magnetometer. The microwave measurements were carried out in a high-Q elliptical copper cavity at four different frequencies corresponding to four different resonant modes: the ${}^e\text{TE}_{111}$ mode at 9.1GHz, the ${}^e\text{TE}_{112}$ mode at 12.8GHz, the ${}^e\text{TE}_{211}$ mode at 15.1GHz and the ${}^e\text{TE}_{113}$ mode at 16.7GHz. The sample was mounted on a sapphire sample holder and placed in the center of the resonator. In that position, the sample lies in a microwave *electric* field E_{mw} maximum in modes ${}^e\text{TE}_{111}$ and ${}^e\text{TE}_{113}$ and in a microwave *magnetic* field H_{mw} maximum in modes ${}^e\text{TE}_{112}$ and ${}^e\text{TE}_{211}$. The temperature was varied between 5 and 50 K, and the applied DC magnetic field between 0 and 16 T. Directly measured quantities are the Q -factor and the resonant frequency f of the cavity loaded with the sample. The Q -factor was measured by a

modulation technique described elsewhere.¹⁷ The empty cavity absorption ($1/2Q$) was subtracted as background from the measured data: the presented experimental curves therefore display changes occurring exclusively in the physical properties of the samples themselves. An automatic frequency control (AFC) system was used to track the source frequency always in resonance with the cavity. Thus, the frequency shift could be measured as the temperature of the sample or the static magnetic field were varied. The two measured quantities represent the complex frequency shift $\Delta\tilde{\omega}/\omega = \Delta f/f + i\Delta(1/2Q)$.

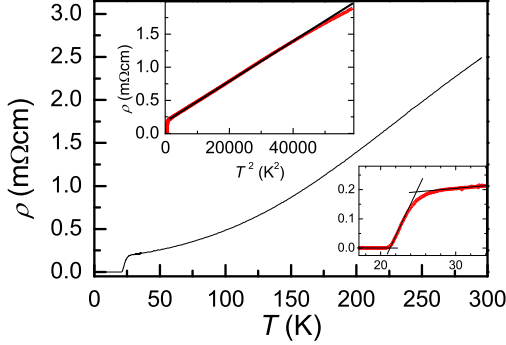


FIG. 1: (Color online) temperature dependence of the resistivity; top left hand side inset: resistivity plotted versus T^2 , showing a deviation above $T \approx 200$ K; bottom right hand side inset: the superconducting transition.

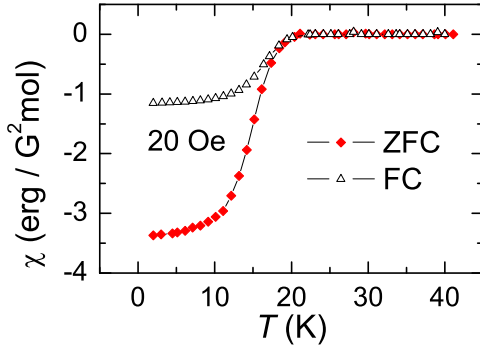


FIG. 2: (Color online) temperature dependence of the susceptibility measured in zero field (ZFC) and in applied magnetic field (FC, 20Oe).

The temperature dependence of resistivity and susceptibility are shown in Fig. 1 and Fig. 2 respectively. Remarkably, the normal state resistivity has a quadratic temperature dependence up to about 200K. The mid-point of the resistive transition yields $T_c = 23.7$ K with a width $\Delta T \approx 4$ K (90% - 10% criterion), while the onset of diamagnetism from the susceptibility curve (ZFC) becomes discernible below $T \approx 22$ K. Both data sets reveal a sample with some degree of inhomogeneity, with a fluorine content slightly different from the nominal value of 0.1. The field-cooled (FC) susceptibility shows significant flux penetration for fields as low as 20 Oe. The two

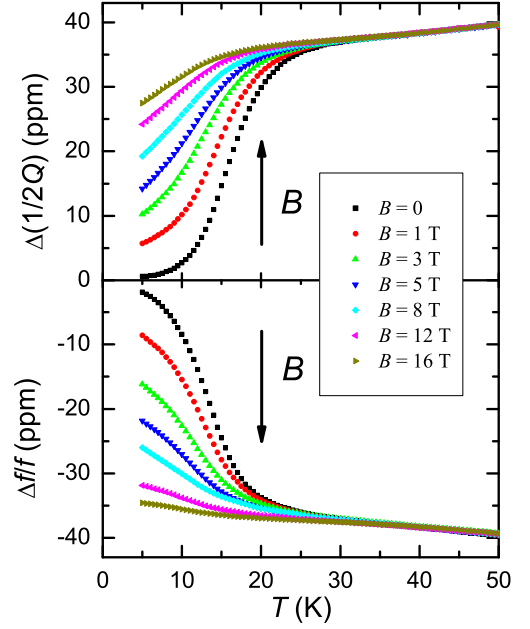


FIG. 3: (Color online) temperature dependence of the complex frequency shift in various applied magnetic fields: imaginary part in the top panel and real part in the bottom panel.

panels of Fig. 3 show the measured complex frequency shift for various values of the applied DC magnetic field in the microwave mode eTE_{112} . For a thick sample there is a proportionality between the complex frequency shift and the surface impedance: $Z_s \propto -i\Delta\tilde{\omega}/\omega$. The factor of proportionality can be determined from the normal state resistivity $\rho_n(T = 30\text{K}) = (0.20 \pm 0.05) \text{ m}\Omega\text{cm}$. From the surface impedance one can determine the complex penetration depth $\tilde{\lambda} = \lambda_1 - i\lambda_2$ through¹⁸

$$Z_s = i\mu_0\omega\tilde{\lambda}. \quad (1)$$

The resulting temperature dependencies of λ_1 and λ_2 in zero applied magnetic field are shown in Fig. 4. In

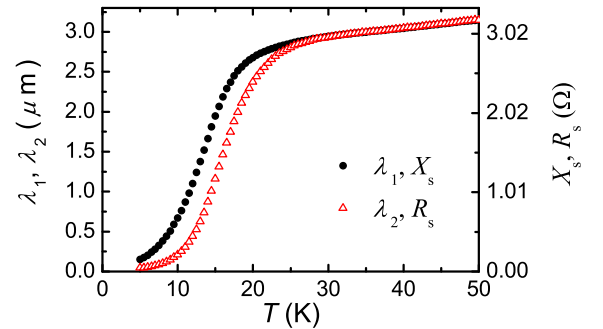


FIG. 4: (Color online) temperature dependence of the complex penetration depth (left axis) and the complex impedance (right axis) in zero applied magnetic field.

the normal state one has $\lambda_1 = \lambda_2 = \delta_n/2$, where δ_n is the normal metal skin depth. In the opposite limit

($T \rightarrow 0$), where the real part of the complex conductivity $\tilde{\sigma} = \sigma_1 - i\sigma_2$ disappears, the complex penetration depth becomes real and identical to the London penetration depth $\lambda_L = \lambda_1(T = 0)$. This analysis was performed for all four microwave modes leading to an estimate of the penetration depth at $T = 5$ K to be $\lambda_1 = (200 \pm 50)$ nm. This is an effective value for the polycrystalline sample and can be taken as the upper limit of the intrinsic value of the London penetration depth in the ab plane. It is clear from Fig. 4 that $\lambda_1(T)$ does not saturate at 5 K; for a nodal order parameter, it would have a linear dependence at very low temperatures¹⁹ due to the gradual excitation of quasiparticles from the superconducting condensate. By linearly extrapolating $\lambda_1(T)$ down to 0 K, a value substantially smaller than 200 nm for the zero temperature London penetration depth would be obtained. From the data in Fig. 3 the upper critical field B_{c2} can be estimated. An empirical criterion for the onset of superconductivity at a given applied field would be the deviation from the apparently linear (normal state) behaviour of the absorption in the top panel of Fig. 3. This method, however, is not very precise, and we therefore decided to apply a quantitative, arguably more rigorous, way of determining such a point. From the complex frequency shift one can extract the complex conductivity $\tilde{\sigma} = \sigma_1 - i\sigma_2$; the emergence of σ_2 is the sign of the establishment of the coherent superconducting state. In Fig. 5 we have plotted the upper critical fields determined by the criterion that σ_2 exceeds 1% of the normal state σ_n . The solid line is the plot of the following formula derived from Ginzburg-Landau theory²⁰

$$B_{c2}(T) = B_{c2}(0) \frac{1 - t^2}{1 + t^2}, \quad (2)$$

where $t = T/T_0$, with $T_0 = 23.0$ K and $B_{c2}(0) = 56$ T. The slope of $B_{c2}(T)$ near T_c , $dB_{c2}(T)/dT$, is -2.5 T/K; this value is substantially unaffected if a different criterion (percentage) for the onset of superconductivity from microwave measurements is adopted. We have neglected in the fit the points above $T_c = 23.7$ K, the critical temperature as deduced from resistivity measurements. Taking these points into account (points that may possibly only be representative of crystallites with a slightly higher T_c) would lead to a somewhat smaller value of B_{c2} but more importantly to an underestimate of the slope of $B_{c2}(T)$ near T_c . We have also measured the field dependence of the complex frequency shift at several constant temperatures. We could not observe the low field signal changes typical of intergrain Josephson junctions. It therefore appears that the preparation of the sample under 1 GPa pressure resulted in a very compact granular structure. From this frequency shift the mixed state effective complex conductivity can be analytically extracted. The effective conductivity^{18,21,22} in an oscillating electric field is given by:

$$\frac{1}{\tilde{\sigma}_{\text{eff}}} = \frac{1 - \frac{b}{1 - i(\omega_0/\omega)}}{(1 - b)(\sigma_1 - i\sigma_2) + b\sigma_n} + \frac{1}{\sigma_n} \frac{b}{1 - i(\omega_0/\omega)}. \quad (3)$$

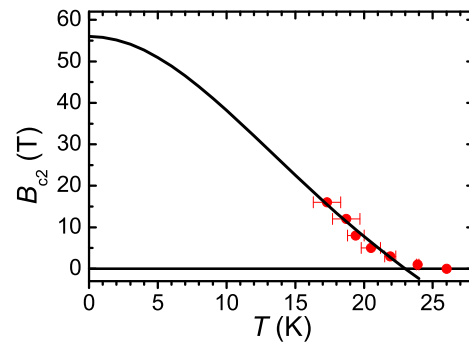


FIG. 5: (Color online) the upper critical field as extracted from the temperature dependence of the complex conductivity in an applied magnetic field; the line is a fit to the data below $T_c = 23.7$ K using equation 2.

The parameter b represents the volume fraction of the sample occupied by the normal vortex cores. ω_0 is the depinning frequency which depends on sample, field and temperature, ranging from the strongly pinned case ($\omega_0 \gg \omega$) to the flux flow limit ($\omega_0 \ll \omega$), where ω is the driving microwave frequency. By numerical inversion

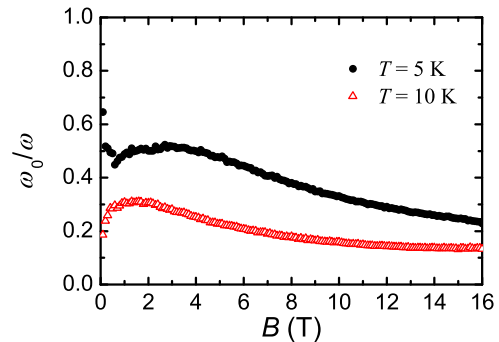


FIG. 6: (Color online) the field dependence of the depinning frequency ω_0 at two temperatures. The driving frequency was $\omega = 2\pi 12.77$ GHz.

of Eq. (3), we have determined the values of b and ω_0 . For the driving frequency $\omega = 2\pi 12.77$ GHz, the field dependence of ω_0/ω is plotted in Fig. 6. The highest value of the depinning frequency $f_0 = \omega_0/(2\pi)$ is obtained for $T = 5$ K at low fields: $f_0 \approx 6$ GHz. With increasing field, and/or temperature, f_0 decreases. Thus, most of the microwave measurements are close to the flux-flow regime.

The normal state resistivity reveals a reasonably good metal ($\rho_0 \approx 200 \mu\Omega\text{cm}$, $\text{RRR} = \rho(300\text{K})/\rho(30\text{K}) = 12.1$) with $\rho \sim T^2$ up to $T \approx 200$ K. This feature is remarkable, but indeed more experimental evidence is needed to prove this to be a signature of Fermi liquid behavior. Our measured effective penetration depth (an upper limit to the London penetration depth) is somewhat smaller than the value of $\lambda_{ab}(0)$ measured by μSR experiments on $\text{LaFeAsO}_{0.9}\text{F}_{0.1}$ ²³; with a value for $\lambda_{\text{eff}}^{-2} \geq 25 \mu\text{m}^{-2}$, this would position our compound

closer than previous results to the line of the electron-doped cuprates on the Uemura plot.^{23,24} Note that our measurement does not rely on any assumption regarding the distribution and arrangement of the vortex lattice within the sample in order to extract λ_{eff} . The obtained values of upper critical field, $B_{c2}=56\text{T}$, and slope near T_c , $dB_{c2}(T)/dT = -2.5\text{T/K}$, are in substantial agreement with other resistivity measurements: for compounds with nominally the same doping, Zhu *et al* obtain the same value of B_{c2} and a similar slope ($dB_{c2}(T)/dT = -2.3\text{T/K}$) using formula 2 for their fit,²⁵ while Hunte *et al* obtain B_{c2} in the range 62-65T and a similar slope by applying the conventional one-band Werthamer-Helfand-Hohenberg theory.²⁶ Their result is closer to that reported by Fuchs *et al* on As-deficient $\text{LaFeAsO}_{0.9}\text{F}_{0.1}$ samples,²⁷ whose value of $dB_{c2}(T)/dT$ near T_c though is considerably larger. The measurement of the depinning frequency yields $f_0 \approx 6\text{GHz}$: a number well into the microwave range. Typically, copper based high- T_c superconductors have depinning frequen-

cies slightly higher than 10GHz ,²⁸ while the depinning frequencies in classical bulk superconductors are below 100MHz .²⁹ This result therefore also points to a substantial communality of features between these novel materials and the cuprates.

In summary, microwave surface impedance measurements on the novel superconductor $\text{LaFeAsO}_{0.9}\text{F}_{0.1}$ provide estimates of the upper critical field ($B_{c2}=56\text{T}$) and the penetration depth ($\lambda_{\text{eff}} \leq 200\text{nm}$); the latter appears to be substantially smaller than the values estimated from measurements carried out by other techniques.^{23,25} Together with the large value of the depinning frequency ($f_0 \approx 6\text{GHz}$), these results yield a phenomenological picture of this system that closely resembles that of the high- T_c cuprate superconductors.

We thank S.-L. Drechsler, G. Fuchs and I. Vekhter for their valuable comments. We acknowledge financial support from the Croatian Ministry of Science, Education and Sports (project no. 119-1191458-1022 “Microwave Investigations of New Materials”).

-
- ¹ Y. Kamihara, T. Watanabe, M. Hirano and H. Hosono, *J. Am. Chem. Soc.* **130**, 3296-3297 (2008).
 - ² Z. A. Ren, W. Lu, J. Yang, W. Yi, X. L. Shen, Z. C. Li, G. C. Che, X. L. Dong, L. L. Sun, F. Zhou and Z. X. Zhao, *Chin. Phys. Lett.* **25**, 2215 (2008); R. H. Liu, G. Wu, T. Wu, D. F. Fang, H. Chen, S. Y. Li, K. Liu, Y. L. Xie, X. F. Wang, R. L. Yang, L. Ding, C. He, D. L. Feng and X. H. Chen, *arXiv:0804.2105v3*.
 - ³ I.I. Mazin, D.J. Singh, M.D. Johannes, and M.H. Du, *arXiv:0803.2740*.
 - ⁴ D.J. Singh and M.-H. Du, *arXiv:0803.0429v1*.
 - ⁵ S. Raghu, X.-L. Qi, C.-X. Liu, D.J. Scalapino and S.-C. Zhang, *arXiv:0804.1113*.
 - ⁶ I. Eremin and M. M. Korshunov, *arXiv:0804.1793*.
 - ⁷ P. A. Lee and X. G. Wen, *arXiv:0804.1739*.
 - ⁸ H. Eschrig, *arXiv:0804.0186v2*.
 - ⁹ L. Boeri, O.V. Dolgov and A.A. Golubov, *arXiv:0803.2703v1*.
 - ¹⁰ C. de la Cruz, Q. Huang, J. W. Lynn, Jiying Li, W. Ratcliff II, J. L. Zarestky, H. A. Mook, G. F. Chen, J. L. Luo, N. L. Wang and P. Dai, *Nature* **453**, 899 (2008).
 - ¹¹ H.-H. Klauss, H. Lütken, R. Klingeler, C. Hess, F.J. Litterst, M. Kraken, M.M. Korshunov, I. Eremin, S.-L. Drechsler, R. Khasanov, A. Amato, J. Hamann-Borrero, N. Leps, A. Kondrat, G. Behr, J. Werner and B. Büchner, *arXiv:0805.0264v1*.
 - ¹² G. Mu, X. Zhu, L. Fang, L. Shan, C. Ren and H.-H. Wen, *arXiv:0803.0928v2*.
 - ¹³ L. Shan, Y. Wang, X. Zhu, G. Mu, L. Fang and H.-H. Wen, *arXiv:0803.2405*.
 - ¹⁴ C. Ren, Z.-S. Wang, H. Yang, X. Zhu, L. Fang, G. Mu, L. Shan and H.-H. Wen, *arXiv:0804.1726v1*.
 - ¹⁵ H.-J. Grafe, D. Paar, G. Lang, N. J. Curro, G. Behr, J. Werner, J. Hamann-Borrero, C. Hess, N. Leps, R. Klingeler and B. Büchner, *arXiv:0805.2595v1*.
 - ¹⁶ S.-L. Drechsler, M. Grobosch, K. Koepf, G. Behr, A. Köhler, J. Werner, A. Kondrat, N. Leps, Ch. Hess, R. Klingeler, R. Schuster, B. Büchner and M. Knapf, *arXiv:0805.1321v1*.
 - ¹⁷ B. Nebendahl, D.-N. Peligrad, M. Požek, A. Dulčić, and M. Mehring, *Rev. Sci. Instrum.* **72**, 1876 (2001).
 - ¹⁸ M. W. Coffey and J. R. Clem, *Phys. Rev. Lett.* **67**, 386 (1991); M. W. Coffey and J. R. Clem, *Phys. Rev. B* **46**, 11757 (1992).
 - ¹⁹ W. N. Hardy, D. A. Bonn, D. C. Morgan, R. Liang, and K. Zhang, *Phys. Rev. Lett.* **70**, 3999 (1993).
 - ²⁰ M. Tinkham, *Introduction to superconductivity*, McGraw Hill, New York, USA, 2nd edition, 1996;
 - ²¹ E. H. Brandt, *Phys. Rev. Lett.* **67**, 2219 (1991).
 - ²² A. Dulčić and M. Požek, *Physica C* **218**, 449 (1993); A. Dulčić and M. Požek, *Fizika A (Zagreb)* **2**, 43 (1993).
 - ²³ H. Lütken, H.-H. Klauss, R. Khasanov, A. Amato, R. Klingeler, I. Hellmann, N. Leps, A. Kondrat, C. Hess, A. Köhler, G. Behr, J. Werner and B. Büchner, *arXiv:0804.3115v1*.
 - ²⁴ A. J. Drew, F. L. Pratt, T. Lancaster, S. J. Blundell, P. J. Baker, R. H. Liu, G. Wu, X. H. Chen, I. Watanabe, V. K. Malik, A. Dubroka, K. W. Kim, M. Rössle and C. Bernhard, *arXiv:0805.1042v1*.
 - ²⁵ X. Zhu, H. Yang, L. Fang, G. Mu, H. Wen, *arXiv:0803.1288*.
 - ²⁶ F. Hunte, J. Jaroszynski, A. Gurevich, D. C. Larbalestier, R. Jin, A.S. Sefat, M.A. McGuire, B.C. Sales, D.K. Christen, D. Mandrus, *Nature* **453**, 903 (2008).
 - ²⁷ G. Fuchs, S.-L. Drechsler, N. Kozlova, G. Behr, A. Köhler, J. Werner, K. Nenkov, C. Hess, R. Klingeler, J.E. Hamann-Borrero, A. Kondrat, M. Grobosch, M. Knapf, J. Freudenberger, B. Büchner, and L. Schultz, *arXiv:0806.0781*.
 - ²⁸ M. Golosovsky, M. Tsindlekht, H. Chayet, D. Davidov, *Phys. Rev. B* **50**, 470 (1994); M. Golosovsky, M. Tsindlekht, and D. Davidov, *Supercond. Sci. Technol.* **9**, 1 (1996).
 - ²⁹ J. I. Gittleman and B. Rosenblum, *Phys. Rev. Lett.* **16**, 734 (1966).